Multi-level Trainable Segmentation for Measuring Gestational and Yolk Sacs from Ultrasound Images

Dheyaa Ahmed Ibrahim(✉), Hisham Al-Assam, Sabah Jassim, and Hongbo Du

Department of Applied Computing, University of Buckingham, Buckingham, UK
Dheyaa.Ibrahim@buckingham.ac.uk

Abstract. As a non-hazardous and non-invasive approach to medical diagnostic imaging, ultrasound serves as an ideal candidate for tracking and monitoring pregnancy development. One critical assessment during the first trimester of the pregnancy is the size measurements of the Gestation Sac (GS) and the Yolk Sac (YS) from ultrasound images. Such measurements tend to give a strong indication on the viability of the pregnancy. This paper proposes a novel multi-level trainable segmentation method to achieve three objectives in the following order: (1) segmenting and measuring the GS, (2) automatically identifying the stage of pregnancy, and (3) segmenting and measuring the YS. The first level segmentation employs a trainable segmentation technique based on the histogram of oriented gradients to segment the GS and estimate its size. This is then followed by an automatic identification of the pregnancy stage based on histogram analysis of the content of the segmented GS. The second level segmentation is used after that to detect the YS and extract its relevant size measurements. A trained neural network classifier is employed to perform the segmentation at both levels. The effectiveness of the proposed solution has been evaluated by comparing the automatic size measurements of the GS and YS against the ones obtained gynaecologist. Experimental results on 199 ultrasound images demonstrate the effectiveness of the proposal in producing accurate measurements as well as identifying the correct stage of pregnancy.

Keywords: Ultrasound image segmentation · Gestational sac · Yolk sac · Trainable segmentation · Pregnancy stage identification

1 Introduction

Medical imaging has unparalleled value in clinical analysis and plays a critical role in the development of effective medical interventions for the treatment of health conditions [1]. Numerous imaging devices have been constructed for diagnostic purposes, and each is characterized by the way in which it draws on different methods in the composition of images. Diagnostic sonography, as an example, operates by transmitting high-frequency sound waves and registering its reflection through a transducer [2]. Given its high-degree of safety and non-invasive nature, ultrasound scanning is routinely employed during pregnancy to monitor growth and health status of foetus.

M. Valdés Hernández and V. González-Castro (Eds.): MIUA 2017, CCIS 723, pp. 86–97, 2017.
DOI: 10.1007/978-3-319-60964-5_8

Statistical evidence reveals that a range of complications occur during pregnancy, the most prevalent of which is miscarriage. Miscarriages are quite common. In the UK, the figure reaches to nearly a quarter of a million each year [3, 4]. As reported in [3], around 20% of all pregnancies are miscarried prior to 24 weeks, and the majority of these occur in the first trimester (namely, within 12 weeks after conception). Gestational assessments conducted over the course of the first trimester tend to focus on the confirmation of fundamental details regarding the pregnancy – namely, whether it has taken place and additionally how many pregnancies there are – and other details addressed include the location of the gestation sac (GS) and the embryo's health status. An assessment of the dimensions of the GS and the Yolk Sac (YS) provides information regarding the probable gestational age of an early pregnancy, and such assessments are also valuable in diagnosing the extent to which the pregnancy is viable. In cases where the Mean Sac Diameter (MSD) of an empty GS greater than 25 mm is observed,the pregnancy will most likely end up as a miscarriage [5]. The value of MSD is generated from the 3 diameters of the GS in combination with the 3 diameters measured in the sagittal and transverse planes [6]. The same process of scan is repeated at the later stage when the yolk sac is starting to grow to further check the status of the pregnancy. As detailed in [5], another indicator of miscarriage is a smaller GS than anticipated based on the gestational age when compared to the last menstrual period. All the descriptions above indicate the necessity of obtaining accurately measured GS and YS sizes.

It is critical to acknowledge that the quality of diagnostic accuracy based on manual measurements can be affected by inconsistency among the measurements obtained by different gynaecologists and even the same gynaecologist, known as inter- and intra-observer variabilities [7]. Therefore, the potential for positive impacts on the result from the provision of automated tools for the enhancement of diagnostic accuracy is clear. Specifically, a computer-based framework to segment and classify ultrasound images could effectively enhance decision-making in pregnancy diagnostics. Additionally, one of the most beneficial prospects associated with the development of this framework would be saving time and resources. Nevertheless, it must be acknowledged developing an automated diagnostic mechanism based on ultrasound images for miscarriage detection is not a straightforward task.

This paper outlines an automatic system for a trainable multi-level segmentation of the GS and the YS based on neural network classifier followed by the measurement of the MSD. After a first level segmentation of the GS, histogram analysis is used to identify the pregnancy stages by establishing whether the GS is empty or not (i.e. it contains the YS). A second level of segmentation is then applied to detect the YS based on the Hough transform followed by producing the MSD. The experimental results upon a dataset of 199 images confirm that the proposed framework on the one hand yields the automatic measurements for the GS and the YS in terms of MSD very close to the gynaecologist measurements without inter- and intra-observer variabilities, and on the other hand achieves an accuracy of pregnancy stage identification around 97.48%.

The rest of the paper is organized as follows: Sect. 2 sets the scene by briefly describing the medical background and the literature review. In Sect. 3 we introduce our approach for identify the pregnancy stage and extract the GS and YS followed by

MSD measurements. Then, Sect. 4 discusses the experiment result. Finally, Sect. 5 concludes the paper and outlines several possible extensions of our approach.

2 Background and Related Work

A regular pregnancy takes 40 weeks (±2 weeks). The first indicator of pregnancy is the absence of the menstrual period. Pregnancy tests, which are conventionally conducted using urine sample, capitalize on the presence or absence of Human Chorionic Gonadotropin (hCG) [8]. In situations where pregnancy tests of this kind yield positive results, an initial scan is conducted to identify the GS's age and, based on this, to calculate the birth date. As being observable in Fig. 1, the structural anatomical elements of early pregnancy are as follows: **(i)** Amniotic sac is a bag of clear fluid inside the uterus where the foetus starts to develop and grow [9]; **(ii)** GS is a structure that surrounds an embryo, in the very early stages of pregnancy (see Fig. 1(b)); **(iii)** Yolk sac is the ring-shaped structure identified within the gestational sac (see Fig. 1(c)) [9]. Heartbeat inside embryo will be seen along with the yolk sac. Failure to identify fatal heartbeat is a sign of abnormal pregnancy which may lead to miscarriage later [9]. Figure 1(d) shows the embryo attached to the YS inside the GS.

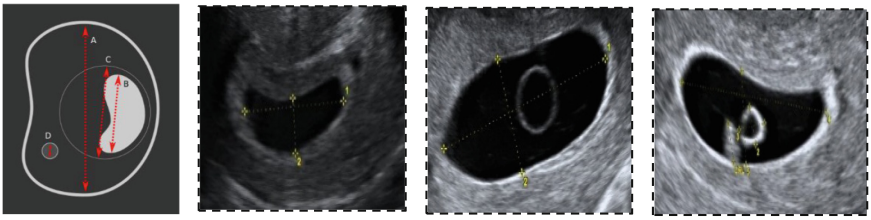

Fig. 1. Examples shows the ultrasound images of a very beginning of pregnancy until developing the embryo (a) The anatomical structures of the early pregnancy A: Gestational sac (GS), B: Crown rump length (CRL) of embryo, C: Amniotic sac and D: Yolk sac (b) Gestational Sac (c) YS within GS (d) embryo attached with YS within GS

The initial structural element that is observable inside the GS is the YS, and an observation of this serves as a confirmation of an intrauterine pregnancy. At the point where the MSD of the GS is 5–6 mm, the YS can be observed by employing transvaginal ultrasound, and it must always be visualized in cases where the MSD of the GS is 8 mm or higher [10].

Early miscarriages are defined as taking place prior to 12 weeks (namely, in the first trimester of pregnancy), while late miscarriages arise in the period from 13–24 weeks. Such phenomena emerge as a consequence of the discontinuation of embryonic development and, in combination with this, the simultaneous discontinuation in the regular development and growth of the GS.

When pregnancy tests yield positive results, it is conventionally the case that the initial scan will be conducted once 12 weeks have elapsed since conception. Scans are

provided at an earlier date in certain circumstances: for example, where vaginal bleeding is reported etc. [10]. The assessment of pregnancy within these first 12 weeks is critical for practitioners because it facilitates the evaluation of the foetus (in terms of development, growth, and health status) and the estimation of a birth date [11, 12].

As mentioned previously, the first measurable sign of an early pregnancy are the geometric characteristics of the GS. The first feature calculated is the MSD. Different studies consider that miscarriage should be declared based on different cut-off values for MSD within the range of 13–25 mm [13, 14]. As displayed below, the most up-to-date limits for miscarriage diagnosis are as follows (Miscarriage identification cut-offs according to the NICE guideline):

- Mean gestational sac diameter (MSD) of ≥ 25 mm with no obvious YS
- Mean sac diameter of (GS and YS) of ≥ 25 and no embryo defined in YS

The segmentation of ultrasound images is crucial for the identification of regions of interest (ROI), one of which, for example, is the GS. Nevertheless, the speckle noise found in ultrasound images (speckles being the cause of the noisy and textured backdrop which results from the reflection and scattering of sound waves inside target tissue) is a chief contributor to the decrease in segmentation accuracy.

Several academic initiatives have directed their efforts towards the issue of ultrasound medical image analysis in the recent 10 years. In a particularly notable study, the researchers outlined an automated system for the measurement of GS dimensions [15]. This system relied on a variety of methods to generate accurate figures for GS age and birth date. Other prominent researchers formulated a new way in which to assess the MSD of the GS using 2-dimensional ultrasound video [16]. The novel method relied on the following series of elements: training, detecting, indexing, and measuring. The chief contributions of these studies stem from their provision of novel frameworks by which the detection of miscarriage can be facilitated in an automated manner; moreover, the studies draw on novel indicators to reinforce diagnostic decision-making. Nevertheless, despite the valuable nature of these studies, a fully-automated miscarriage indicator identification framework which employs ultrasound images is still lacking; as previously alluded to, this is a product of the way in which noise complicates the attempt to automatically segment ROIs, thereby meaning it must be conducted manually or semi-automatically [3, 4]. Hence, the present author is alert to the fact that this paper represents the first attempt to outline a fully-automatic system for the identification of pregnancy stage and segmentation of GS with YS.

3 The Proposed Method

Figure 2 provides an overview of the system for the automatic identification of the pregnancy stage as well as detecting and measuring the GS and the YS from a static B-mode image. The framework consists of a sequence of steps starting from segmenting and measuring the GS, followed by automatically identifying the stage of pregnancy, and finally segmenting and measuring the YS. Each step of the framework will be explained in details in the following sub-sections.

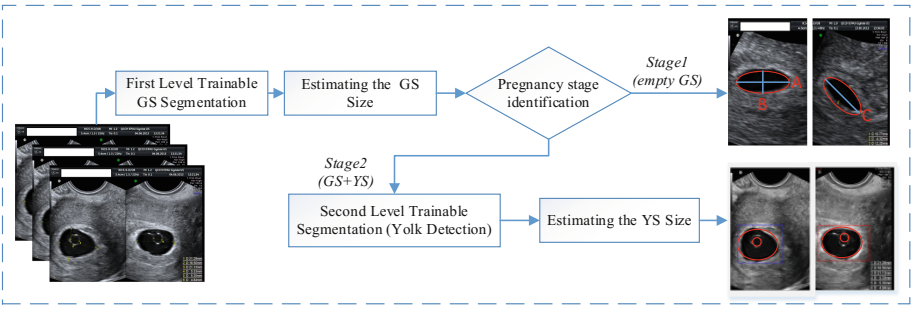

Fig. 2. General framework for the automatic segmentation

3.1 First Level Trainable GS Segmentation

The aim of the first level segmentation is to isolate the GS from the rest of the image. The process starts by first selecting a certain number of images as training images. From each training image, a number of samples, i.e. a small window of square regions of a certain size (e.g. 3×3), are taken from the inside of the GS (Class 1) and outside the GS (Class 2). For each window of either class, a set of HOG features (to be described in later) are extracted. The labelled feature vectors collected from all samples are then used to train a neural network classifier. Once training is complete, each image from the testing set is used as an input for the segmentation algorithm. The algorithm scans an image pixel by pixel. For each pixel, a small square region of the same window size with the pixel as the centre is constructed, and the HOG feature of the region is extracted and classified by the trained neural network as being inside the GS or outside GS. If the region is inside a GS, the central pixel is also labelled as inside the GS; otherwise outside the GS. Once all pixels of the image are labelled, the region of the "inside pixels" is taken as the segmented GS.

The central problematic element associated with this stage of the process stems from the fact that upon the application of the trainable segmentation, binary objects remain which resemble the sac. Consequently, it is necessary for a fully automated system to first detect these objects and consequently remove them. This process of filtration takes place in accordance with the non-sac objects' characteristics such as circularity, area, and the greyscale mean [2].

The histogram of oriented gradients (HOG) is a feature descriptor that facilitates the identification of objects in digital images. HOG was formulated for the quantification of gradient orientation occurrences in localised image sections, and have been well documented in [17, 18]. The process of HOG feature extraction involves taking a window around the pixels called cells. The mask [−1,0, 1] is used to computing image gradients. In our adaptation of this extraction method (see Fig. 3), for orientation binning, we directly used the gradient at each image locations for the corresponding orientations. The orientation cells are chosen in the range of 0–180^{o} with 9 bins. For better invariance to illumination, shadowing, etc., contrast-normalization of the local histogram is applied.

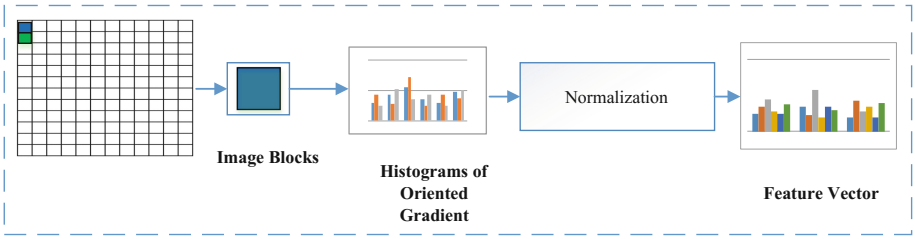

Fig. 3. HOG process

3.2 Estimating the GS Size

As explained earlier, each GS is viewed in two perpendicular planes. The GS usually seems to be more elliptical at the early stages, therefore, our system aims to locate the best-fitted ellipse for the segmented GS for each plane. The region props function in Matlab is utilized to fit an ellipse to the GS. Four parameters can be returned by this process. These are major axes, minor axes, Centroid and Orientation. The GS is presumably has an ellipsoidal shape in 3D, the three main dimensions of the ellipsoid has generally been calculated by the minor and major dimension from the sagittal plane and the major dimension from the transverse plane. The average of the three Dimension is taken as the MSD.

3.3 Histogram Analysis to Identify the Pregnancy Stage

This stage aims to establish if the GS is empty or not i.e. whether it contains a YS inside. To do this, first, the binary image resulted from the GS segmentation step is used as a mask to locate the pixels inside the GS from the original image. Histogram analysis is applied to those pixels to determine whether theYS is present within the GS or not by following the process outlined in Fig. 4.

Consider that the grey-level histogram matches with a GS, f (x, y), constituted of light objects (the YS's border) superimposed on a dark backdrop (the GS). Furthermore, the configuration is organized such that the pixels of the object and backdrop display grayscale levels are categorized into a pair of dominant modes. If this is the case, the immediately discernible method by which the border of the YS can be estimated from the GS involves the selection of a threshold (T) that facilitates the separation of these modes. Consequently, a pixel (x, y) according to which f (x, y) > T (based on bin frequency) can be designated as a YS border.

Under certain circumstances, when the frequency is high within GS, it does not necessarily mean there is a YS: the frequency simply serves to denote small noise objects. Consequently, for each bin with frequency greater than T, pixels of the intensity represented by the bin are located in the GS image (see Fig. 4). A post-processing check is conducted to see if the pixels form an object. If not, the GS is considered as empty (stage1); otherwise, the GS contains YS (stage2).

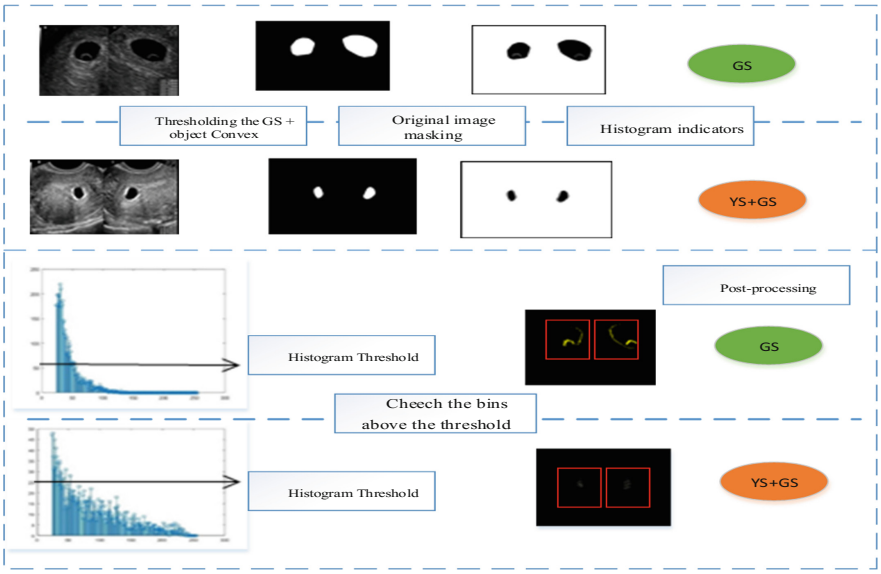

Fig. 4. Histogram analysis to identify the pregnancy stages

3.4 Second Level Trainable Segmentation: Estimating the YS Border

Once the histogram analysis of the area inside the GS establishes the existence of the YS, a second level trainable segmentation is employed at this stage to estimate the YS border. The main challenge here is that in certain scenarios, the YS's border is vague and unclear, which means that techniques based on the pixel intensity thresholding cannot work satisfactorily. The machine learning based approach has more promises in such situations.

A pixel feature (in accordance with the pixel neighbourhood) is used to identify the border pixels. The training phase is implemented by selecting window of size N × N for each yolk boundary and non-boundary in image (see Fig. 5). The testing phase will process only the pixels which are inside the GS sac using the mask from the GS segmentation stage. The output of this stage is a binary GS include the GS with white colour and the YS border with black colour.

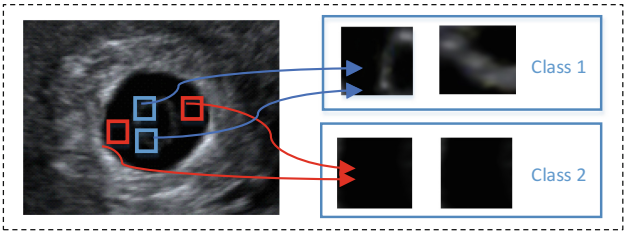

Fig. 5. Select samples for the learning phase

Once the second level trainable segmentation estimates the YS border. A convex hull is employed to facilitate the delineation of the YS from the GS. The rationale for this is of three folds: (i) it facilitates the maintenance of the entire GS and the assessment of the MSD; (ii) it allows just the YS's border to be retained for the Hough transform stage; and (iii) reduces the frequency of objects in conjunction with the likelihood of object circularity, thereby capturing the YS. All the objects inside the convex will be as input to the circle Hough transform to detect the best circle next.

3.5 Locating YS and Measuring its Size

Based on the assumption that a circle exists in (x and y)space, the image coordinates, and that the YS's perimeter points have been acquired, a circle in the (a and b) parameter space corresponds to every point on the circle's perimeter. The (a and b) space constitutes a circle accumulation of the input image for a specified radius (r) (see Fig. 6). The critical piece of information when attempting to identify a circle is the radius, and this is because it determines circle dimensions in the (a and b) space. In cases where a circle constructed in the (a and b) space is not identical in size to the initial circle's radius, the former will not contact at a single location. Hence, a suitable radius means that the constructed circles will contact at a single location, and this constitutes the centre circle identified in the image coordinates. Assuming the YS has acircle shape in 3D, the two principal axes of the circle can be estimated by the radius (R1) of the circle from the sagittal plane and the radius (R2) of the circle from the trans-verse plane. The ((2*R1 + R1)/3) will be taken as the MSD.

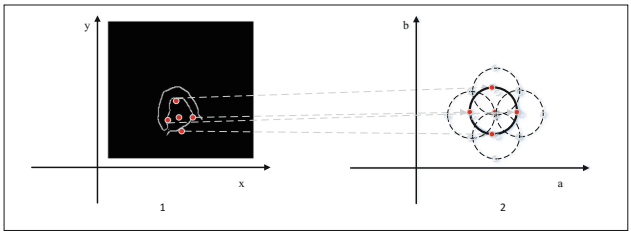

Fig. 6. (1) Circle located on parameter plane *x*,*y*, (2) transform in space *a*,*b*

4 Experiments and Results

4.1 Dataset

The dataset consists of 199 ultrasound images, 184 of which are of an empty GS (157 PUV and 27 miscarriage). The remaining 15 are for GSs with YSs inside. The images were acquired in 3 dataset batches, with the first constituted of 94 images; the second constituted of 90; and the third constituted of 15 with GS and YS. The images are obtained by the Early Pregnancy Unit, Imperial College Healthcare Trust, London. The visualisation of the GS and YS for each image was conducted from a pair of viewpoints:

namely, the sagittal and transverse planes. The images were accompanied with manually-obtained diameters (D_1, D_2, and D_3) together with the resulting MSDs in addition to diagnostic outcomes.

4.2 Experimental Protocol

A 2-layer backpropagation neural network has been used in each of the two segmentation levels. In the first level, the network was trained with 100 sample regions obtained from 8 training images. In the second level of segmentation, the network was trained with 60 sample regions obtained from 3 images due to the limited number of images in batch 3.

It is important to recognize that the features extracted and the quality of segmentation are directly influenced by the block size, i.e. the size of the window around the pixel. As shown in Fig. 7, when the block size is small, more pixels outside the real region of interest are considered as "inside" pixels. This will results in the creation of more irrelevant objects outside the real object of interest, increasing the level of difficulty for removing those objects later (Fig. 7(b)). As the block size increases, fewer pixels outside the object of interest would be confused as "inside" pixels, and hence fewer irrelevant objects are created (Fig. 7(c, d)). However, when the block size gets too large, the possibility that a block contains pixels of both "inside" and "outside" also increases, resulting imprecise classification of the pixel class (Fig. 7(d)). As such, to ensure high-quality segmentation, the block size must be determined carefully. Based on our observation, the block size of 5 × 5 seems optimal.

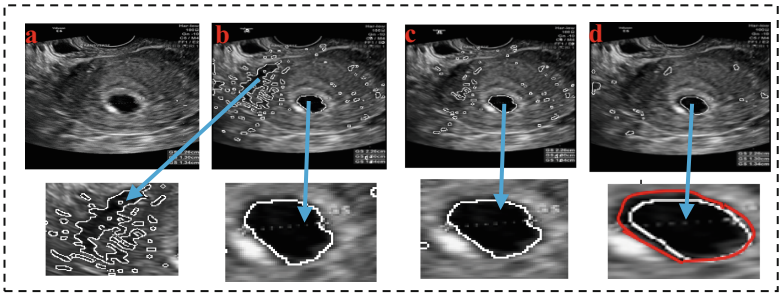

Fig. 7. Trainable segmentation result, (a) original image, (b) segmented image with window size 3*3, (c) segmented image with window size 5*5, (b) segmented image with window size 7*7. The wait line represent the automatic segmentation and the red color represent the manual segmentation. (Color figure online)

The effectiveness of the proposed method was evaluated by conducting examinations at the following phases: (i) evaluate the pregnancy stage identification accuracy based on the segmentation of GS; (ii) assess the segmentation precision by comparing the automatic and manual measurement results of MSD.

4.3 Results

Pregnancy Stages Identification

We are interested in the effectiveness of histogram thresholding and the histogram thresholding followed by post-processing in the proposed method as explained in Sect. 3.3. Two experiments were conducted: one for using the thresholding alone, and the other for using thresholding followed by post-processing. Figure 8 shows that an overall average accuracy of 84.42% with stage1 identification (empty GS) of 83.69% and stage2 identification (GS &YS) of 100% for can be achieved in the first set of the experiment (Histogram threshold). By contrast, an overall accuracy of 97.48% with stage1 identification of 97.28% and with stage2 identification of 100% was achieved in the second experiment as (Histogram threshold with post-processing). The results confirm that the second method approved that the threshold of the histogram is not enough to estimate if there is a YS or not.

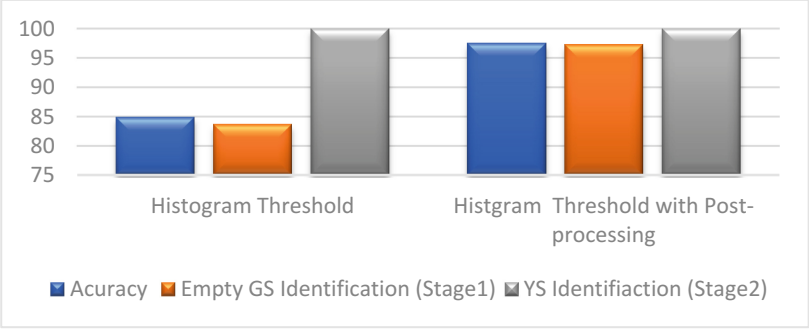

Fig. 8. Pregnancy stage identification

Segmentation Result (Manual vs. Automatic Measurements)

The manual calculation of the proportion of successful GS segmentations was conducted with the human visual system (HVS). Regarding batches 1 and 2, it was noted that 153/184 GS images were segmented which is 83.15%.

Additionally, out of the 15 images in the third batch, GS were segmented precisely, which is 100%. Furthermore, the YS segmentation was successful for 14 out of the 15 images, i.e. 93.3%. To facilitate the provision of a suitable system assessment regarding the subsequent phases, each image associated with unsuccessful segmentation of GS was not included.

Automatic MSD measurements were considered in relation to manual measurements to assess the degree to which the proposed system was effective. Figure 9 provides an indication of the performance. Figure 9a illustrates the result of batch 1 and batch 2 (Empty GS). Figure 9b represents the result for batch three where the points inside the red ellipse represent the measurement for YS and the other points represents the GS measurements. In view of the approximately 45° regression line, it can be concluded that the automatic measurements are very close to the manual measurements. It can also be observed that there is no apparent systematic bias of the automatic measurements.

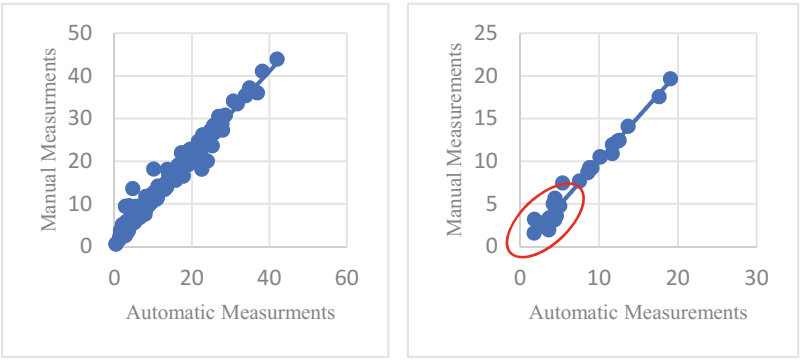

Fig. 9. Comparison manual and automatic MSD measurements. (a) Empty GS (b) GS + YS

5 Conclusion

The purpose of this study was to outline and evaluate a new approach to automatic identification the pregnancy stage and segmentation of the GS and YS from B-mode static ultrasound images. This paper argued that the segmentation of such images is a challenging task due to overlap between colour intensities of the GS and YS with surrounding tissues.

The proposed automatic system overcome these difficulties by formulating a multi-level framework: (1) first-level trainable GS segmentation to locate the GS sac; (2) using histogram properties of the GS to identify the pregnancy stage; (3) second level of trainable segmentation is used to segment and measure the YS. Finally, the MSD for the YS and the GS were extracted. Experiments showed that the automatic measurements were very close to the manuals ones extracted by domain experts which confirms the viability of the proposal.

Our future work includes extending the test of our method on more images, improving the efficiency of the proposed method, and investigate the effectiveness of alternative image-based indicators such as those extracted from the border of the GS.

Acknowledgements. Many thanks to all the collaborators involved in this work. Department of Early Pregnancy, Imperial College, Professor Tom Bourne and Dr. Jessica Farren for their help in preparing the images and all important information related to the datasets used in this study.

References

1. Lee, L.K., Liew, S.C.: A survey of medical image processing tools. In: 2015 4th International Conference on Software Engineering and Computer Systems (ICSECS) (2015)
2. Ibrahim, D.A., Al-Assam, H., Du, H., Farren, J., Al-karawi, D., Bourne, T., Jassim, S.: Automatic segmentation and measurements of gestational sac using static B-mode ultrasound images. In: SPIE Commercial + Scientific Sensing and Imaging (2016)

3. Khazendar, S., Al-Assam, H., Bourne, T., Jassim, S.A.: Automatic identification of early miscarriage based on multiple features extracted from ultrasound images. In: MIUA (2014)
4. Preisler, J., Kopeika, J., Ismail, L., Vathanan, V., Farren, J., Abdallah, Y., Battacharjee, P., Van Holsbeke, C., Bottomley, C., Gould, D., et al.: Defining safe criteria to diagnose miscarriage: prospective observational multicentre study (2015)
5. Ectopic Pregnancy and Miscarriage: Diagnosis and Initial Management. National Institute for Health and Care Excellence (NICE) (2012). Accessed 2015
6. Pexsters, A., Luts, J., Van Schoubroeck, D., Bottomley, C., Van Calster, B., Van Huffel, S., Abdallah, Y., D'Hooghe, T., Lees, C., Timmerman, D., et al.: Clinical implications of intra-and interobserver reproducibility of transvaginal sonographic measurement of gestational sac and crown–rump length at 6–9 weeks' gestation. Ultrasound Obstet. Gynecol. **38**(5), 510–515 (2011)
7. Doubilet, P.M., Benson, C.B., Bourne, T., Blaivas, M.: Diagnostic criteria for nonviable pregnancy early in the first trimester. N. Engl. J. Med. **369**(15), 1443–1451 (2013)
8. Creighton University Medical Center, Omaha Nebraska. Diagnostic and Interventional Radiology Department/Ultrasound of Early Pregnancy. Creighton University Medical Center (2013). http://web.archive.org/web/20070814054851/http:/radiology.creighton.edu/pregnancy.htm#section4
9. Uideline, L.: Ultrasound evaluation of first trimester pregnancy complications. J. Obstet. Gynaecol. Can. **27**(6), 581–585 (2005)
10. Khazendar, S., Farren, J., Al-Assam, H., Du, H., Sayasneh, A., Bourne, T., Jassim, S.: Automatic Identification of Miscarriage Cases Supported by Decision Strength Using Ultrasound Images of the Gestational Sac (2015)
11. Geirsson, R., Busby-Earle, R.: Certain dates may not provide a reliable estimate of gestational age. BJOG: Int. J. Obstet. Gynaecol. **98**(1), 108–109 (1991)
12. Kaur, A., Kaur, A.: Transvaginal ultrasonography in first trimester of pregnancy and its comparison with transabdominal ultrasonography. J. Pharm. Bioallied Sci. **3**(3), 329 (2011)
13. Bourne, T.: Why greater emphasis must be given to getting the diagnosis right: the example of miscarriage. Australas. J. Ultrasound Med. **19**(1), 3–5 (2016)
14. Levi, C., Lyons, E., Lindsay, D.: Ultrasound in the first trimester of pregnancy. Radiol. Clin. North Am. **28**(1), 19–38 (1990)
15. Chakkarwar, V., Joshi, M.S., Revankar, P.S., et al.: Automated analysis of gestational sac in medical image processing, pp. 304–309 (2010)
16. Zhang, L., Chen, S., Li, S., Wang, T.: Automatic measurement of early gestational sac diameters from one scan session. In: SPIE Medical Imaging, p. 796342. International Society for Optics and Photonics (2011)
17. Dalal, N., Triggs, B.: Histograms of oriented gradients for human detection. In: 2005 IEEE Computer Society Conference on Computer Vision and Pattern Recognition (CVPR 2005) (2005)
18. Patil, M.S.S., Junnarkar, M.A., Gore, M.D.: Study of texture representation techniques. image **3**(3), 267–274 (2014)